IAI Journals.ASM.org

Pertussis Toxin Exacerbates and Prolongs Airway Inflammatory Responses during *Bordetella pertussis* Infection

Carey E. Connelly,[a] Yezhou Sun,[b] and Nicholas H. Carbonetti[a]

Department of Microbiology and Immunology,[a] and Institute for Genome Sciences,[b] University of Maryland School of Medicine, Baltimore, Maryland, USA

Throughout infection, pathogenic bacteria induce dramatic changes in host transcriptional repertoires. An understanding of how bacterial factors influence host reprogramming will provide insight into disease pathogenesis. In the human respiratory pathogen *Bordetella pertussis*, the causative agent of whooping cough, pertussis toxin (PT) is a key virulence factor that promotes colonization, suppresses innate immune responses during early infection, and causes systemic disease symptoms. To determine the full extent of PT-associated gene regulation in the airways through the peak of infection, we measured global transcriptional profiles in the lungs of BALB/c mice infected with wild-type (WT) or PT-deficient (ΔPT) *B. pertussis*. ΔPT bacteria were inoculated at a dose equivalent to the WT dose and at a high dose (ΔPT^{high}) to distinguish effects caused by higher bacterial loads achieved in WT infection from effects associated with PT. The results demonstrated that PT was associated with a significant upregulation of immune and inflammatory response genes as well as several other genes implicated in airway pathology. In contrast to the early, transient responses observed for ΔPT^{high} infection, WT infection induced a prolonged expression of inflammatory genes and increased the extent and duration of lung histopathology. In addition, the administration of purified PT to ΔPT^{high}-infected mice 1 day after bacterial inoculation exacerbated and prolonged inflammatory responses and airway pathology. These data indicate that PT not only is associated with exacerbated host airway responses during peak *B. pertussis* infection but also may inhibit host mechanisms of attenuating and resolving inflammation in the airways, suggesting possible links between PT and pertussis disease symptoms.

Bacterial toxins disrupt a broad range of eukaryotic cell functions, causing changes in host physiology that often underlie severe disease pathology. For the human respiratory pathogen *Bordetella pertussis*, multiple toxins act in concert to facilitate the adhesion, survival, and proliferation of bacteria within the airways (48). Among these toxins, pertussis toxin (PT) has emerged as a key virulence factor for its ability to promote bacterial colonization (17), modulate host immune responses (14), cause systemic effects (53, 56), and, possibly, boost transmission (52). Previous studies using infant mice associated PT with lethal *B. pertussis* infection (31, 85), and in humans, *B. pertussis* strains that lack functional PT display reduced pathogenicity (10). Despite its well-established role as a virulence factor, mechanistic links between PT and pertussis disease symptoms have not been well defined.

Pertussis can be fatal in infants (62), and it hampers patients of all ages with a range of symptoms, the most severe of which include pneumonia, pulmonary hypertension, encephalopathy, and the hallmark paroxysmal cough (whooping cough) that can last for weeks or even months after bacterial clearance (48). The incidence of pertussis is highest in developing nations, accounting for 90 to 95% of the estimated 16 million worldwide cases and 195,000 deaths in 2008 (87). In developed countries, reemergent pertussis has sparked significant public health concerns in recent years, where the efficacy of widespread vaccination programs seems to be waning (33). Interestingly, the characterization of resurgent pertussis in some countries highlights *B. pertussis* strains with increased promoter activity at the *ptx* locus (52), suggesting that higher levels of PT contribute to increased virulence in these strains.

At the molecular level, PT modifies inhibitory G proteins, effectively uncoupling signaling through cognate receptors. PT is a secreted exotoxin of the AB_5 configuration, comprised of one active subunit (S1) and a pentameric binding oligomer (77). After interactions with glycosylated molecules on the surface of mammalian cells (49, 86), PT undergoes endocytosis and retrograde trafficking to the endoplasmic reticulum (ER), where the active subunit dissociates and enters the cytoplasm (66). S1 catalyzes the ADP-ribosylation of the $G_i\alpha$ and $G_o\alpha$ subunits (37, 54, 81), preventing the G-protein activation required for subsequent adenylyl cyclase inhibition and other downstream effects. ADP-ribosylation activity accounts for many of the reported effects of PT, but the B oligomer can also affect signaling through binding properties (3, 36, 60).

A comparison of wild-type (WT) and PT-deficient (ΔPT) strains in mouse models of *B. pertussis* infection indicates that PT heightens virulence through the modulation of host immune responses. PT confers a colonization advantage to WT bacteria such that within 24 to 48 h postinoculation, mice infected with WT *B. pertussis* have a 10- to 50-fold-higher bacterial load in their lungs than mice inoculated with equal numbers of the ΔPT strain (17). This difference arises primarily from the PT-mediated inhibition of resident airway macrophages, as clodronate liposome depletion of macrophages prior to infection restores colonization by the ΔPT strain to WT levels (18). In addition, PT interferes with the chemotaxis of multiple cell types *in vitro* and *in vivo* (4, 22, 76). In

Received 1 August 2012 **Returned for modification** 29 August 2012
Accepted 20 September 2012
Published ahead of print 1 October 2012
Editor: J. L. Flynn
Address correspondence to Nicholas H. Carbonetti, ncarbone@umaryland.edu.
Supplemental material for this article may be found at http://iai.asm.org/.

doi:10.1128/IAI.00808-12

the case of neutrophils, PT reduces early influx into the mouse respiratory tract by suppressing the expressions of genes for the neutrophil-attracting chemokines keratinocyte-derived chemokine (KC) and lipopolysaccharide-induced CXC chemokine (LIX) and macrophage inflammatory protein 2 (MIP-2) (4). The inhibitory functions of PT extend to adaptive immunity, where it was shown to suppress the serum antibody response to *B. pertussis* (16), decrease the expression and cell surface levels of antigen-presenting molecules (47, 73), suppress the induction of regulatory T cells (20), and decrease the antibody-mediated clearance of bacteria (41).

In addition to the immunosuppressive functions described above, several lines of evidence implicate PT in heightened inflammatory responses. When used as an adjuvant, PT promotes experimental autoimmune diseases (2, 57, 92), and recent studies showed that PT induces the development of Th17 cells (5, 19, 35), now recognized as major contributors to autoimmune pathogenesis (84). Previous studies reported increased gamma interferon (IFN-γ) and tumor necrosis factor alpha (TNF-α) secretion by lymphocytes, splenocytes, and macrophages in response to PT (64, 82, 91). In addition, at the peak of *B. pertussis* infection, PT enhances neutrophil influx into the airways through the upregulation of interleukin-17 (IL-17) and the neutrophil-attracting chemokines (5).

Because G proteins play an integral role in diverse cellular processes, we hypothesized that PT would induce multiple effects on the host respiratory tract during *B. pertussis* infection, including the upregulation of inflammatory responses. Our results present the first global, *in vivo* evaluation of host transcriptional responses affected by PT in the context of pertussis infection. The results reveal that PT activity is associated with an extensive upregulation of inflammatory genes at the peak of infection and highlight several genes that may contribute to pertussis-evoked airway pathology and disease. In addition, our results reveal the novel finding that PT increases the extent and duration of inflammatory responses and pathology in lungs of *B. pertussis*-infected mice.

MATERIALS AND METHODS

Bacterial strains. The WT, ΔPT, and PT* *B. pertussis* strains used in this study are streptomycin- and nalidixic acid-resistant derivatives of Tohama I (17). The ΔPT strain does not produce PT due to an in-frame deletion spanning all 5 PT genes (17). The PT* strain produces enzymatically inactive toxin, as it carries two amino acid substitutions in the S1 subunit (R9K and E129G) that abrogate ADP-ribosylation activity (65). All *B. pertussis* strains were grown on Bordet-Gengou (BG) agar plates supplemented with 10% defibrinated sheep blood and 200 μg/ml streptomycin.

Mouse infections. Six- to eight-week old female BALB/c mice (Charles River Laboratories) were anesthetized with inhaled isoflurane and intranasally (i.n.) inoculated with 50 μl of either sterile phosphate-buffered saline (PBS) or a suspension of *B. pertussis* in PBS. Inocula contained approximately 1×10^6 CFU of WT, ΔPT, or PT* bacteria for the normal dose or 1.5×10^7 to 4×10^7 CFU (WT^{high}, ΔPT^{high}, and PT^{*high}) for high-dose experiments. In selected experiments, mice received intranasal treatment with 50 μl PBS or 50 μl purified PT (100 ng) at 24 h postinoculation. At the indicated times postinoculation, mice were euthanized by carbon dioxide inhalation followed by thoracotomy. Unless otherwise stated, the lungs were intracardially perfused with 5 ml of sterile PBS. For analyses of bacterial counts, the trachea and right lung (cranial, medial, caudal, and postcaval lobes) were dissected, immersed in 2 ml of sterile PBS, and homogenized. Serial dilutions of homogenates were plated onto BG blood agar plates with 200 μg/ml streptomycin, and CFU were determined by counting colonies after 4 to 5 days of growth at 37°C. Lung tissue for other purposes was collected as described below. Animal procedures were performed according to a protocol approved by the University of Maryland Baltimore (UMB) Institutional Animal Care and Use Committee.

RNA isolation and processing. After the perfusion of the lungs, the left lobe was removed and immediately frozen in a dry-ice–ethanol bath. RNA was extracted by using RNA Stat60 (TelTest, Inc.). Each frozen lung sample was homogenized immediately after the addition of Stat60 (1 ml per 75 to 100 mg tissue) by using an Omni TH mixer (Omni, Inc.). Homogenates were incubated for 4 min at room temperature to allow nucleoprotein complexes to dissociate and were combined with 200 μl chloroform. After gentle mixing (1 min), rest at room temperature (1 min), and centrifugation, 400 μl of the aqueous phase was mixed with 500 μl isopropanol and stored at −20°C for 1 to 2 h. After precipitation and centrifugation, pellets were washed with 80% ethanol, dried briefly in a DNA Speedvac instrument (Savant), and resuspended in 50 μl H_2O. The concentration of each sample was determined by using a NanoDrop spectrophotometer (ND-1000; Thermo Scientific). Twenty-five micrograms of RNA was combined with 10 μl RDD buffer (Qiagen), 2.5 μl DNase (Qiagen), and distilled water (dH_2O) up to a final volume of 100 μl and incubated at 25°C for 10 min. DNased samples were subsequently purified by using the RNeasy minikit (Qiagen), and final concentrations were determined by using the NanoDrop ND-1000 spectrophotometer. For quantitative real-time PCR (qPCR), cDNA was generated from 1 μg of RNA by using a reverse transcription system (Promega) with random primers. For microarray hybridization, RNA quality was determined by using an Agilent 2100 Bioanalyzer. cRNA was prepared from 150 ng of RNA by using the Illumina TotalPrep RNA amplification kit. The transcription reaction mixture to generate cRNA was incubated for 14 h at 37°C.

Microarray processing and statistical analysis. Individual cRNA samples were hybridized onto Illumina MouseRef8_v2.0 bead array chips containing 25,697 probes ($n = 3$ per group for samples from infected mice, and $n = 2$ for PBS-treated mice). Sample probe profiles were extracted and normalized by the median method implemented in the beadarray R package (25). Differential expression analysis was performed on normalized data by using the limma R package (75) to compare gene expression profiles among different time points and infection strains. All lists were filtered to include only probes with a false discovery rate (FDR) of ≤0.05 and a fold change (FC) of ≥1.5. The FDR represents the expected proportion of false-positive results in a set of significant hypotheses (9). Functions and pathways relevant to significant probes were assigned by using Ingenuity Pathway Analysis (IPA) (Ingenuity Systems) functional and pathway annotations, with *P* values calculated by using Fisher's exact test.

Quantitative real-time PCR. qPCR was carried out by using the 7500 Fast real-time PCR system (Applied Biosystems) and Fast SYBR green master mix (catalog number ABI4385617). Each reaction mixture contained the following: 12.5 μl SYBR green mix, 6 μl H_2O, 0.75 μl each forward and reverse primers (0.3 μM final concentration), and 5 μl cDNA (~300 ng). Primer sequences were obtained from the Universal ProbeLibrary for mouse (Roche Applied Science), from qPrimerDepot (NCBI), or were designed to flank an intron and yield a cDNA-based product with a length of between 60 and 130 bp. Primer sequences can be found in Table S1 in the supplemental material. Relative gene expression changes were calculated by using the $\Delta\Delta C_T$ method, and the mouse housekeeping gene hypoxanthine phosphoribosyltransferase (HPRT) was used for expression normalization.

Bronchoalveolar lavage fluid and neutrophil counts. A 20-gauge blunt-ended needle was inserted into a small incision toward the top of the trachea in euthanized mice and tied in place with surgical thread. Bronchoalveolar lavage (BAL) was performed by flushing the lungs twice with 0.7 ml of sterile PBS (1.4 ml PBS total). In lungs used for the collec-

tion of BAL fluid cells as well as the isolation of RNA, equivalent proportions of lung tissue and BAL fluid cells were combined prior to the freezing of samples for RNA extraction (one-sixth of the total lung tissue with one-sixth of the isolated BAL fluid cells). Aliquots of BAL fluid were used for cell counting on a hemocytometer and for cytospin centrifugation. Cytospin slides were stained with modified Wright's stain, and 200 to 800 cells from multiple microscope fields were counted and identified.

Pathology. After euthanasia by carbon dioxide inhalation, the lungs and trachea were exposed via dissection. The right bronchiole was tied off by using suture string, a piece of the caudal lobe was collected for RNA isolation, and the rest of the right lobes were dissected for bacterial load determinations. Subsequently, 0.35 ml of 4% paraformaldehyde (PFA) was intratracheally perfused into the left lobe. The trachea was tied shut to allow the fixation of the lung in an inflated state. The inflated left lobe was dissected from the thoracic cavity and fixed in 4% PFA for 60 h at 4°C. Paraffin-embedded sections of lung tissue were prepared at the UMB Histology Core and stained with hematoxylin and eosin. Histopathological evaluations were conducted by a pathologist at the University of Maryland Baltimore with experience evaluating rodent lungs who was blinding to experimental conditions. Sections were given a score of between 0 and 5 in the following categories: peribronchiolar inflammation, perivascular inflammation, epithelial cell damage, edema, hemorrhage, and numbers of eosinophils, neutrophils, macrophages, and lymphocytes. Reported pathology scores reflect the sum of these values for each mouse.

Cytokine ELISA. Tissue for protein analysis was collected immediately after euthanasia, without lung perfusion. The cranial, medial, and caudal lobes of the right lung were collected into 2 ml of ice-cold PBS, and the left lobe was collected into PBS–2% bovine serum albumin (BSA)–0.5% Triton X-100. After homogenization, serial dilutions of samples from the right lung were plated onto BG agar with streptomycin to determine CFU per lung. Left lobe homogenates were centrifuged twice (17,000 × *g* at 4°C for 5 min) to remove cells and debris. Supernatants were collected into a separate tube, aliquoted, and stored at −80°C. An enzyme-linked immunosorbent assay (ELISA) was performed at the UMB Cytokine Core Laboratory.

Statistical analysis. Statistical analysis was performed on log-transformed data by using GraphPad Prism for Macintosh 4.0c (GraphPad Software, San Diego, CA). Student's two-tailed, unpaired *t* test was used for comparing 2 groups. For comparisons of 3 or more groups, data were analyzed by using one-way analysis of variance (ANOVA) followed by Bonferroni's multiple-comparison posttest for pairwise comparisons.

Microarray data accession number. Raw and normalized data sets were deposited into the NCBI Gene Expression Omnibus database under accession number GSE33995.

RESULTS

Microarray analysis of lung transcriptional responses to WT and PT-deficient *B. pertussis*. To further understand the effects of PT on host airway responses during *B. pertussis* infection, we carried out genome-wide expression arrays for mice infected with either WT or PT-deficient *B. pertussis* bacteria. Groups of BALB/c mice were intranasally inoculated with PBS, 1.3×10^6 CFU of the WT, or 1.3×10^6 CFU of the ΔPT strain (WT with PT genes deleted) (Fig. 1A). Because PT increases bacterial loads of WT *B. pertussis* by at least 10-fold over those of the ΔPT strain within 1 to 2 days postinoculation (dpi) (17), differential host responses to these infections might arise either directly from the activity of PT or from differences in bacterial loads. Thus, a fourth group of mice was inoculated with a high dose (3.1×10^7 CFU) of the ΔPT strain (ΔPT^{high}) (Fig. 1A) to achieve bacterial loads equivalent to those of the WT through the peak of infection. Infected mice were euthanized at 6 h and at 1, 2, 4, and 7 dpi ($n = 5$ per time point). PBS-treated mice were euthanized at 6 h and at 2 dpi ($n = 3$ per time point). Whole lung tissue was isolated from each mouse,

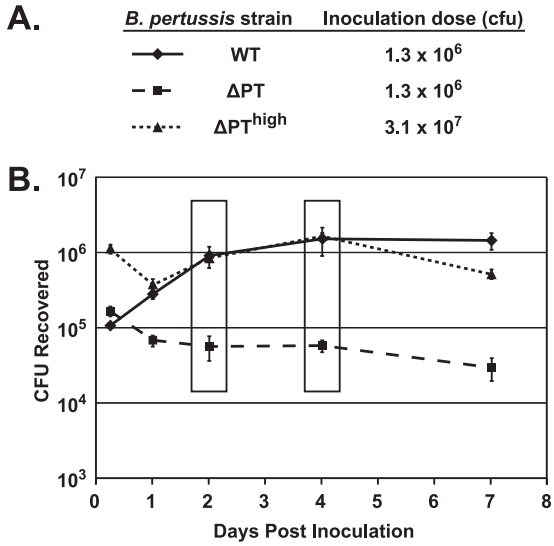

FIG 1 Infection strategy and respiratory tract colonization of mice for genome-wide expression analysis. (A) BALB/c mice (female, 7 weeks of age) were intranasally inoculated with either PBS or the indicated strain and dose of *B. pertussis*: WT and ΔPT. A high dose (24×) of the ΔPT strain (ΔPT^{high}) was used to control for differences in bacterial loads between the WT and low-dose ΔPT infections. (B) Bacterial loads recovered from the lungs of mice at 6 h or 1, 2, 4, or 7 days postinoculation. Graphed values represent mean CFU in three mice ± standard errors of the means. Lungs of PBS-treated control mice were harvested at 6 h and 2 dpi ($n = 5$). RNA was isolated from lungs of all mice, and individual samples at 2 and 4 dpi were processed further for microarray analysis (boxes).

RNA was extracted from the left lobe of each lung, and bacterial counts per animal were determined from homogenates of the trachea plus right lung lobes. Bacterial loads were equivalent in the lungs of WT- and ΔPT^{high}-infected mice at 1, 2, and 4 dpi (Fig. 1B), with peak numbers being reached by day 4. As observed previously (15, 17), there were significantly fewer ΔPT strain cells in mouse airways after inoculation with the lower dose, demonstrating the important role of PT in promoting bacterial infection in this model.

Previously, we found that PT inhibited early (1 dpi) neutrophil recruitment to the lungs of *B. pertussis*-infected mice, but by 4 dpi, PT activity was associated with increased neutrophil influx and the expression of neutrophil-recruiting chemokines (4, 5). We reasoned that PT may be associated with additional proinflammatory responses at the peak of infection and that the transition to this proinflammatory stage might result from changes both prior to and at day 4. Thus, global gene expression patterns in individual mouse lung samples at 2 and 4 dpi were assessed by microarray analysis, using the Illumina MouseRef8_v2.0 platform to screen for over 24,000 mouse transcripts. Microarray data were analyzed via multiple comparisons at each time point, with most efforts being focused on the discovery of PT-associated changes in host gene expression levels. Infected mice were compared to mock-infected mice, WT- and ΔPT^{high}-infected mice were compared to ΔPT-infected mice, and WT-infected mice were compared to ΔPT^{high}-infected mice. All resulting lists were filtered to include only those genes with statistically significant differential expression levels (false discovery rate [FDR] of ≤0.05 and fold change [FC] of ≥1.5).

Summary of comparisons. The total number of genes regu-

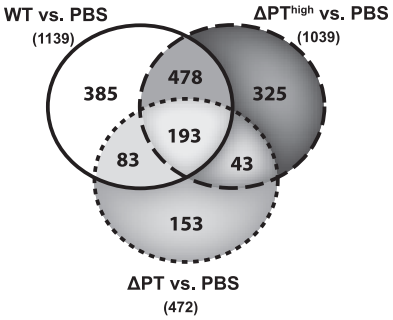

	WT	ΔPT	ΔPT^{high}
≥ 2 fold	270	47	361
≥ 4 fold	39	3	46

FIG 2 Global gene expression level changes in mouse lung during infection with WT or PT-deficient *B. pertussis*. cDNA generated from lung samples harvested at 2 and 4 dpi was hybridized onto Illumina Mouse Ref8_v2.0 chips carrying probes for >24,000 mouse genes. The diagram shows numbers of unique and common differentially regulated probes between WT-infected (solid circle), ΔPT-infected (dashed circle), and ΔPT^{high}-infected (dotted circle) mice compared to PBS-treated mice. The total number of genes regulated during each infection at either time point is shown in parentheses below each label. The table shows the number of genes regulated at least 2- and 4-fold for each comparison. Data reflect probes with an FDR of ≤0.05 and a fold change of ≥1.5.

lated in the lung during each *B. pertussis* infection was determined by comparisons to values for mice inoculated with PBS (Fig. 2). WT-infected mice displayed 1,139 differentially expressed genes (including 270 genes with changes of more than 2-fold and 39 with changes of more than 4-fold). Infection with the ΔPT strain induced the fewest changes, with differences detected by only 472 probes (47 genes with changes of more than 2-fold and 3 with changes of more than 4-fold). A total of 1,039 differences were observed for ΔPT^{high}-infected mice (361 genes with changes of more than 2-fold and 46 with changes of more than 4-fold). To validate the array data, qPCR measurements were performed for selected genes from the RNA samples used in the microarray analysis to assess relative transcript abundances and expression changes over time. Results from the qPCR analysis were consistent with those of the microarray analysis, although for some genes, qPCR detected fold changes of a greater magnitude than those reported by array data (see Table S2 in the supplemental material).

Analyses revealed 193 genes that were differentially expressed (relative to values for PBS-treated mice) in all three infections (Fig. 2; see also Table S3 in the supplemental material). Ingenuity Pathway Analysis (IPA) software was used to identify enriched functions among this group of genes. Highly significant functional categories included "cell death" ($P = 6.55 \times 10^{-6}$), "cell cycle" (3.06×10^{-5}), and "connective tissue development and function" ($P = 1.77 \times 10^{-4}$), indicating that many of these genes function in cell turnover and the structural integrity of lung tissue. Transcripts involved in pro- as well as antiapoptotic responses were affected, including Bcl-binding component 3, CD40, TRAF2, and the transcription regulators SMAD6, IKBA, and FOSB. Several genes involved in cell growth (Wnt2, insulin-like growth factor-binding protein 3, microtubule-associated protein tau, and platelet-derived growth factor receptor B) as well as the maintenance and development of blood vessels (angiopoietin 1, cadherin 5, cysteine-rich protein 1, and gap junction membrane channel protein alpha 5) were downregulated. Furthermore, some changes suggested a trend toward a loss of connective tissue, as transcripts encoding components of the extracellular matrix were downregulated, including collagen types IIIa1 and IVa5, spondin, elastin, gelsolin, perlecan, keratins 10 and 23, as well as a lysyl oxidase enzyme required for the integrity of matrix proteins (45). In addition, cathepsin K, a protease that degrades elastin and collagen, was upregulated. These common changes represent PT-independent effects of *B. pertussis* on host gene expression and suggest a dynamic interplay between cell death and renewal amid infection-induced tissue damage.

The assessment of responses over time revealed a distinct course of gene expression changes for each infection (Table 1). Compared to PBS-treated mice, WT-infected lungs showed moderate changes at 2 dpi (309 genes) and more extensive regulation at 4 dpi (971 genes), with the majority of genes being upregulated. ΔPT-infected lungs displayed moderate changes at both time points, with the regulation of 376 genes at 2 dpi declining to 179 genes at 4 dpi. In contrast, ΔPT^{high}-infected lungs had the highest number of differentially regulated genes at 2 dpi (872 genes), the majority of which were upregulated. This number declined to 379 genes by 4 dpi. Remarkably, a direct comparison of samples from ΔPT^{high}- and ΔPT-infected mice revealed zero significant differences in gene expression levels at 4 dpi (Table 1), despite robust differences at 2 dpi and the disparity in bacterial loads at 4 dpi (Fig. 1B). These data indicate that the high dose of *B. pertussis* elicited a broad, early host response but that, in the absence of PT, these gene expression changes were short lived despite the continued presence of high bacterial loads.

PT-associated transcriptional responses. The 385 genes regulated uniquely in WT infection but not in ΔPT infections (Fig. 2)

TABLE 1 Summary of microarray data comparisons[a]

Infection comparison	No. of genes					
	Day 2			Day 4		
	Upregulated	Downregulated	Total	Upregulated	Downregulated	Total
WT vs PBS	118	191	309	753	218	971
ΔPT vs PBS	121	255	376	108	71	179
ΔPT^{high} vs PBS	662	210	872	223	156	379
WT vs ΔPT	11	0	11	539	43	582
ΔPT^{high} vs ΔPT	792	102	894	0	0	0
WT vs ΔPT^{high}	38	700	738	315	21	336

[a] Genes with an FDR of ≤0.05 and an FC of ≥1.5.

represent changes potentially associated with PT. However, some of these genes did not show significant differences in direct comparisons of WT- to ΔPT- or ΔPT^{high}-infected mice (see Table S4 in the supplemental material). To exclude potential false-positive results and to enrich for true PT-associated genes, we filtered the 385 WT infection-specific genes to include only genes that also displayed significant FC values of ≥1.5 in direct comparisons of WT to ΔPT and WT to ΔPT^{high} infections at both time points. In addition, genes that were regulated in common with the other infections (versus PBS) but for which the WT FC was ≥1.5 times that of the ΔPT or ΔPT^{high} FC were also included in this list. The filtered list contains 91 genes whose regulation was specifically linked with PT production during *B. pertussis* infection (89 upregulated and 2 downregulated) (Table 2). The list reveals numerous genes not previously reported to have an association with PT, including a large cohort of inflammatory response genes and several genes with links to airway pathology, indicating an important role for PT in pertussis disease pathogenesis.

(i) Immune and inflammatory responses. An analysis of the 91 PT-associated genes using IPA showed that immune and inflammatory responses represented the most significantly enriched functions identified at 4 dpi (Fig. 3A; see also Table S5 in the supplemental material). In addition, immune and inflammatory cell signaling pathways dominated the list of top IPA canonical pathways enriched in PT-associated genes (see Table S6 in the supplemental material). Several of the most robustly induced changes involved cytokine and chemokine genes (Table 2), suggesting a major effect of PT on cell recruitment and activation. Transcripts for the neutrophil-attracting chemokines CXCL1 (KC), CXCL2 (MIP-2), and CXCL5 (LIX) displayed some of the greatest fold changes, consistent with our previous report that the expression levels of these chemokines and the influx of neutrophils greatly increase during WT *B. pertussis* infection. PT was also associated with an upregulated expression of the CXCR2 gene (IL-8 receptor), which encodes the primary CXCL1, CXCL2, and CXCL5 receptors (71) and the CSF3 (granulocyte colony-stimulating factor [G-CSF]) receptor, which is involved in neutrophil maturation and mobilization (26). Two members of the IL-6 family of cytokines, IL-6 and oncostatin M (OSM), were upregulated in association with PT as well as the OSM receptor. *In vitro*, PT stimulates IL-6 secretion from dendritic cells, which contributes to the differentiation of cocultured naive $CD4^+$ T cells into Th17 cells (19). The function of OSM during *B. pertussis* infection has not been described, although it was reported to carry profibrotic activities in some pulmonary disorders and matrix-destructive properties in others (55, 68, 70). The expression levels of two IL-1 family cytokines, IL-1β and IL-33, also increased in the presence of PT. IL-1β is associated with disease in multiple inflammatory disorders (8). IL-1β is essential for recovery from *B. pertussis* infection in a mouse model, and PT contributes to IL-1β production by bone marrow-derived macrophages incubated with *B. pertussis* (90). The discovery of IL-33 induction represents a novel finding in the context of PT-associated responses, and it may be interesting in light of its contribution to inflammation and airway pathology in asthma (12). Furthermore, recent studies found that IL-33 production by lung-resident innate lymphoid cells (ILCs) and the IL-33-mediated induction of amphiregulin by ILCs play a crucial role in airway tissue repair after influenza virus infection (51). Our finding that PT increases both IL-33 and amphiregulin expression levels suggests that the upregulation of repair mechanisms may be another important aspect of PT-associated responses in *B. pertussis* infection. Finally, the presence of PT correlated with gamma interferon (IFN-γ) induction as well as the upregulation of interferon-inducible genes (Table 2), including members of a GTPase family recently ascribed an antibacterial function (39). Another IFN-γ-induced host defense involves the limiting of the availability of tryptophan by the induction of enzymes involved in tryptophan metabolism, and the gene for one such enzyme, indoleamine 2,3-dioxygenase, was among the PT-associated genes.

Additional PT-linked proinflammatory responses to *B. pertussis* infection included increased expression levels of transcripts involved in lipopolysaccharide (LPS) signaling, including the LPS receptor CD14, LPS-binding protein (LBP), and a lysophosphatidic acid receptor recently shown to modulate LPS-induced inflammatory responses (93). PT was also correlated with increased expression levels of genes encoding inflammation-associated adhesion molecules, including P-selectin, vascular cell adhesion molecule, and C-lectin type 4e, a sensor for damaged cells expressed on macrophages (89). The increased expression levels of adhesion molecules likely contribute to inflammatory cell recruitment to the lungs.

Amid the numerous proinflammatory responses described above, genes involved in the control of immune responses were also induced in association with PT (Table 2). Homologs of antichymotrypsin (SERPINA3N, -A3F, and -A3G) and two inter-alpha trypsin inhibitors (ITIH1 and ITIH4) were upregulated. SERPINA3N inhibits granzyme B activity (74), mitigating the activity of cytotoxic T lymphocytes and natural killer cells that secrete granzyme B to induce apoptosis. ITIH1 was reported previously to possess anti-inflammatory activity through the inhibition of complement proteins (30). Lipocalin-2, a molecule involved in antimicrobial defense (28), protects against airway inflammation in a mouse model of allergic asthma (23). In addition, the tumor necrosis factor receptor superfamily 9 protein (Tnfrsf9) was shown previously to push the balance between Th17 cells and Tregs in favor of Treg generation (40). Finally, zinc finger protein 36 was reported previously to bind and destabilize cytokine mRNAs to reduce inflammatory responses (13). Therefore, the upregulation of proinflammatory genes associated with PT is potentially balanced by the induction of anti-inflammatory gene expression, which presumably prevents the lethality of this infection.

(ii) Genes implicated in pathology. An analysis of PT-associated transcripts at 4 dpi revealed a significant enrichment of genes that mediate some aspects of airway and pulmonary pathology (Fig. 3B). Specifically, the IPA "airway hyperresponsiveness" (AHR) annotation category ($P < 2.3 \times 10^{-5}$) included the differential regulation of genes for the cytokines IFN-γ and IL-6, the chemokine CCL2, receptors in the leukotriene and TNF receptor families, and the transcription factor SOCS3. CCL2 can activate mast cells, and the administration of CCL2 to mouse airways was shown previously to induce prolonged AHR (88). The leukotriene B4 receptor and IL-1β are linked to the increased synthesis of eicosanoids, such as leukotrienes and prostaglandins, known to induce smooth muscle contraction. In addition, one of the most highly induced PT-associated genes (slc26a4) encodes an anion transporter, pendrin, shown to mediate AHR and inflammation in asthma (58). The gene encoding tissue inhibitor of metalloprotease 1 (TIMP-1) was a highly upregulated PT-associated gene (Table 2). Increased TIMP-1 expression levels have been associ-

TABLE 2 PT-associated gene expression level changes[a]

ID	Gene	WT vs PBS		WT vs ΔPT		WT vs ΔPT^{high}	
		FDR	FC	FDR	FC	FDR	FC
Cytokines and chemokines							
14825	Chemokine (C-X-C motif) ligand 1	0.000	18.2	0.000	18.2	0.000	8.0
16176	Interleukin-1 beta	0.000	11.1	0.000	11.0	0.000	6.0
20311	Chemokine (C-X-C motif) ligand 5	0.000	4.6	0.000	5.4	0.001	4.2
20310	Chemokine (C-X-C motif) ligand 2	0.000	3.2	0.000	2.9	0.000	2.5
77125	Interleukin-33	0.000	3.1	0.000	2.7	0.001	2.7
18413	Oncostatin M	0.000	2.9	0.000	3.1	0.000	2.5
20296	Chemokine (C-C motif) ligand 2	0.000	2.4	0.000	2.5	0.000	2.5
16193	Interleukin-6	0.000	2.3	0.000	2.3	0.001	2.2
15978	Gamma interferon	0.000	1.8	0.004	1.7	0.002	1.7
Other secreted proteins							
16819	Lipocalin 2	0.000	14.0	0.001	8.2	0.008	2.4
76905	Leucine-rich alpha-2-glycoprotein 1	0.000	5.1	0.000	4.5	0.005	2.5
15458	Hemopexin	0.000	3.4	0.000	2.9	0.000	2.2
20201	S100 calcium-binding protein A8 (calgranulin B)	0.000	3.0	0.001	3.6	0.001	2.4
20202	S100 calcium-binding protein A9 (calgranulin B)	0.000	2.6	0.001	3.2	0.000	2.3
11839	Amphiregulin	0.000	2.4	0.009	1.8	0.001	2.3
21923	Tenascin C	0.000	2.0	0.000	1.9	0.001	1.7
16803	Lipopolysaccharide-binding protein	0.000	2.0	0.008	2.2	0.035	1.7
245195	Resistin-like gamma	0.000	1.9	0.001	2.1	0.008	1.5
246316	Leucine-rich repeat LGI family, member 2	0.000	1.6	0.005	1.5	0.005	1.5
71690	Endothelial cell-specific molecule 1	0.000	−1.7	0.000	−2.0	0.041	−2.1
Immune receptors/adhesion molecules							
12475	CD14 antigen	0.000	6.2	0.000	6.5	0.001	3.4
12986	Colony-stimulating factor 3 receptor (granulocyte)	0.000	4.8	0.000	3.3	0.000	3.2
12765	Interleukin-8 receptor, beta	0.000	3.2	0.000	2.9	0.000	2.7
20344	Selectin, platelet	0.000	2.2	0.008	1.8	0.003	1.8
213233	TAP-binding protein-like	0.000	2.1	0.001	1.7	0.002	1.8
14128	Fc receptor, IgE, low affinity II, alpha polypeptide	0.000	1.9	0.004	1.8	0.031	1.6
20343	Selectin, lymphocyte	0.000	1.8	0.003	2.0	0.027	1.6
18414	Oncostatin M receptor	0.000	1.8	0.003	1.8	0.005	1.6
56619	C-type lectin domain family 4, member e	0.001	1.7	0.004	1.7	0.003	1.7
58218	Triggering receptor expressed on myeloid cells 3	0.000	1.6	0.001	1.8	0.002	1.6
Transmembrane proteins							
23985	Solute carrier family 26, member 4	0.000	9.4	0.000	9.3	0.000	5.4
235712	MAS-related GPR, member A2B	0.000	2.5	0.000	2.3	0.001	2.4
21942	Tumor necrosis factor receptor superfamily, member 9	0.000	2.4	0.000	2.2	0.001	1.9
76574	Major facilitator superfamily domain containing 2a	0.000	2.3	0.005	2.2	0.011	1.8
22329	Vascular cell adhesion molecule 1	0.000	1.8	0.000	1.9	0.005	1.8
50930	Tumor necrosis factor superfamily, member 14	0.000	1.8	0.001	1.6	0.004	1.6
11541	Adenosine A2b receptor	0.000	1.8	0.001	1.8	0.015	1.6
20351	Semaphorin 4A	0.000	1.8	0.003	1.7	0.014	1.5
68279	Mucolipin 2 (TRPML1)	0.000	1.7	0.002	1.7	0.005	1.6
14745	Lysophosphatidic acid receptor 1	0.000	1.7	0.004	1.5	0.002	1.6
16995	Leukotriene B4 receptor 1	0.001	1.7	0.005	1.8	0.010	1.5
16404	Integrin alpha 7	0.001	1.5	0.000	1.8	0.004	1.6
68713	Interferon-induced transmembrane protein 1	0.001	1.5	0.004	1.5	0.005	1.5
Enzymes							
15930	Indoleamine 2,3-dioxygenase 1	0.000	3.7	0.000	3.6	0.000	3.1
51797	CTP synthase	0.000	3.1	0.000	2.6	0.001	2.3
626578	Guanylate-binding protein 10	0.000	3.0	0.000	2.8	0.001	2.2
229900	Guanylate-binding protein 7	0.000	2.8	0.000	2.8	0.004	2.3
22375	Tryptophanyl-tRNA synthetase	0.000	2.6	0.000	2.1	0.004	1.8
21816	Transglutaminase 1, K polypeptide	0.000	2.2	0.012	1.8	0.000	2.0
69581	*ras* homolog gene family, member U	0.000	1.9	0.001	1.8	0.007	1.6

(Continued on following page)

TABLE 2 (Continued)

ID	Gene	WT vs PBS		WT vs ΔPT		WT vs ΔPT^{high}	
		FDR	FC	FDR	FC	FDR	FC
71780	Myoinositol 1-phosphate synthase A1	0.000	1.9	0.001	1.9	0.019	1.6
18113	Nicotinamide *N*-methyltransferase	0.000	1.9	0.000	1.8	0.001	1.8
20656	Superoxide dismutase 2, mitochondrial	0.000	1.9	0.001	1.7	0.001	1.7
56045	SAM domain and HD domain, 1	0.000	1.8	0.002	1.6	0.003	1.6
71893	NADPH oxidase organizer 1	0.000	1.8	0.000	2.1	0.039	1.6
14528	GTP cyclohydrolase 1	0.000	1.8	0.000	2.1	0.011	1.6
66725	Leucine-rich repeat kinase 2	0.001	1.8	0.028	1.5	0.016	1.6
223920	Sterol *O*-acyltransferase 2	0.000	1.8	0.004	1.6	0.002	1.6
70025	Acyl-CoA thioesterase 7	0.001	1.8	0.040	1.6	0.044	1.6
19734	Regulator of G-protein signaling 16	0.000	1.7	0.003	1.8	0.002	1.9
56454	Aldehyde dehydrogenase 18 family, member A1	0.000	1.7	0.001	1.6	0.005	1.5
80914	Uridine-cytidine kinase 2	0.001	1.5	0.000	1.8	0.003	1.7
235674	Acetyl coenzyme A acyltransferase 1B	0.004	−1.6	0.003	−2.0	0.014	−1.5
Peptidases							
21929	Tumor necrosis factor, alpha-induced protein 3	0.000	2.0	0.000	2.2	0.015	1.6
240913	ADAMTS4	0.000	1.9	0.000	2.1	0.000	2.0
19186	Proteasome (prosome, macropain) 28 subunit, alpha	0.000	1.8	0.002	1.7	0.011	1.5
17392	Matrix metallopeptidase 3	0.000	1.7	0.005	1.5	0.007	1.5
Protease inhibitors							
21857	Tissue inhibitor of metalloproteinase 1	0.000	10.4	0.000	12.1	0.000	5.0
20716	Serine peptidase inhibitor, clade A, member 3N	0.000	6.8	0.000	7.8	0.000	4.6
16427	Inter-alpha-trypsin inhibitor, heavy chain 4	0.000	5.7	0.000	4.8	0.003	3.5
20715	Serine peptidase inhibitor, clade A, member 3G	0.000	3.7	0.000	2.7	0.008	2.1
238393	Serine peptidase inhibitor, clade A, member 3F	0.000	2.9	0.000	2.5	0.002	2.3
16424	Inter-alpha-trypsin inhibitor, heavy chain 1	0.000	2.3	0.000	2.6	0.000	2.2
433016	Predicted gene 5483	0.000	2.0	0.001	2.4	0.001	2.1
Nuclear proteins							
12702	Suppressor of cytokine signaling 3	0.000	3.4	0.000	3.7	0.000	2.5
16477	Jun-B oncogene	0.000	2.6	0.000	2.4	0.001	1.7
18030	Nuclear factor, interleukin-3 regulated	0.000	2.4	0.000	2.5	0.000	2.4
16362	Interferon regulatory factor 1	0.000	2.4	0.000	2.2	0.000	2.1
80859	Nuclear factor of kappa light polypeptide gene	0.000	2.2	0.000	2.4	0.009	1.6
20846	Signal transducer and activator of transcription 1	0.000	2.2	0.000	2.5	0.005	1.8
22695	Zinc finger protein 36	0.000	2.1	0.004	1.8	0.045	1.5
23882	Growth arrest and DNA-damage-inducible 45 gamma	0.001	2.0	0.005	2.0	0.007	1.9
Structural proteins							
27375	Tight-junction protein 3	0.000	2.3	0.002	1.8	0.010	1.6
78785	CAP-GLY domain-containing protein family, member 4	0.000	1.9	0.000	1.7	0.005	1.5
73710	Tubulin, beta 2B	0.000	1.7	0.011	1.5	0.002	1.5
16906	Lamin B1	0.000	1.7	0.000	2.1	0.008	1.5
Other							
24108	Ubiquitin D	0.000	1.8	0.045	1.6	0.015	1.6
78388	Major vault protein	0.000	1.9	0.001	1.6	0.002	1.6
71982	Sorting nexin 10	0.000	2.2	0.000	2.3	0.007	1.6
56722	LPS-induced TNF-α factor	0.000	1.7	0.001	1.8	0.002	1.8
547253	Poly(ADP-ribose) polymerase family, member 14	0.004	1.7	0.002	2.1	0.036	1.7

[a] ID, NCBI Entrez Gene Identifier; FDR, false discovery rate; FC, fold change (values at 4 dpi); SAM, *S*-adenosylmethionine; HD, histidine and aspartic acid; CoA, coenzyme A; LGI, leucine-rich glioma-inactivated; TAP, transporter associated with antigen processing; GPR, G protein-coupled receptor; ADAMTS, a disintegrin and metalloprotease with thrombospondin motifs; CAP-GLY, cytoskeleton-associated protein, glycine-rich.

ated with reduced pulmonary function (72) and pneumonia (21) but may play a protective role against airway inflammation and hyperresponsiveness (69).

Another symptom of severe pertussis includes pulmonary hypertension (48). PT-specific changes revealed an upregulation of resistin-like gamma (retnlg in mice and RETNLB in humans), which codes for a secreted protein linked to scleroderma-associated pulmonary hypertension in humans (6). RETNLB induces the proliferation of primary human pulmonary smooth muscle and endothelial cells (6) and may contribute to airway remodeling

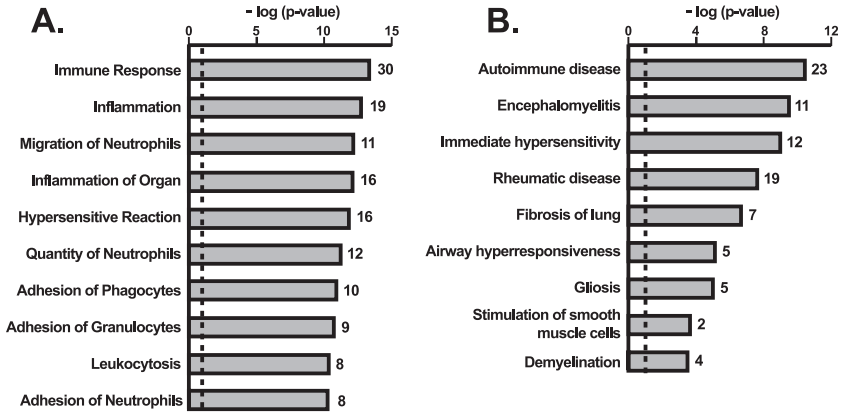

FIG 3 PT-dependent regulation of immune response-related functions. Genes regulated specifically in the presence of pertussis toxin (Table 2) were analyzed by using Ingenuity Pathway Analysis. Graphs show the 10 most significantly enriched overall (A) and pathology-related (B) functional annotations. Numbers to the right of each bar indicate the total number of differentially regulated genes related to a given function. The dashed line indicates a significance threshold of a *P* value of 0.05.

in asthma (27). Pulmonary hypertension can also be associated with compromised connective tissue (32). The "connective tissue disorders" IPA function revealed PT-associated genes that promote connective tissue autoimmune disorders ($P < 3.8 \times 10^{-4}$). Upregulated genes in this category include transcripts for the proteases MMP3 and ADAMST4, known to degrade extracellular matrix components, and for proteins associated with arthritis, including CXCL1, CXCL5, and TIMP1.

Finally, it is possible that an altered signaling of nerves innervating the trachea and bronchi contributes to prolonged cough in pertussis. Interestingly, multiple functions related to neurological disease showed significant enrichment among PT-associated genes, including transcripts involved in encephalomyelitis ($P = 2.97 \times 10^{-10}$), gliosis ($P = 4.44 \times 10^{-5}$) (CCL2, IDO1, IL-6, interferon regulatory factor 1 [IRF1], SELL, SEMA4A, STAT1, TIMP1, TNFSF14, and VCAM1), and axon damage ($P = 4.33 \times 10^{-4}$). In the central nervous system CCL2, IL-6, and IFN-γ can promote demyelination, and IRF1 contributes to pathogenesis in the experimental autoimmune encephalomyelitis (EAE) model of multiple sclerosis (MS) (67). The enrichment of PT-associated genes for these functions is consistent with the frequent usage of PT as an adjuvant to promote EAE (11, 92), the mouse model of MS.

Overall, these data highlight the major stimulatory effect of PT on immune and inflammatory responses during peak infection, indicating the potentially important role that PT may play in pertussis disease pathogenesis.

PT-associated changes in gene expression depend on ADP-ribosylation activity. Previous studies indicated a sufficiency of the PT B oligomer, which lacks the enzymatic activity of the A (S1) subunit, in mediating some effects of PT in other models (3, 36, 60, 78). Therefore, we asked whether the enzymatic activity of PT was required for the altered expression of the PT-associated genes with the highest fold changes. Mice were infected with either WT *B. pertussis* (7.5×10^5 CFU) or a strain producing an inactive form of PT (PT*) with changes to the active site that disrupt the toxin's ability to ADP-ribosylate substrate G proteins. PT* bacteria were inoculated at regular (7.5×10^5 CFU) and high (1.5×10^7 CFU) doses to control for bacterial loads during infection, as discussed above. At 4 dpi, mean bacterial counts in the lungs were 1.8×10^6 CFU in WT-infected mice, 2.4×10^5 CFU in PT*-infected mice, and 2.5×10^6 CFU in PT*^{high}-infected mice (data not shown). In all cases, expression level changes in WT-infected lungs were significantly higher than those induced by infection with the PT* strain at regular or high doses (Fig. 4). In addition, there were no significant differences among these genes between responses to infection with the PT* strain (from this experiment) and responses to infection with the ΔPT strain (from other experiments [data not shown]). These results indicate that the binding of PT is not sufficient to drive some of the highest changes in gene expression levels reported in this array and that a fully active toxin is required.

PT-dependent and -independent time course of inflammatory gene expression. Despite the presence of equal bacterial loads

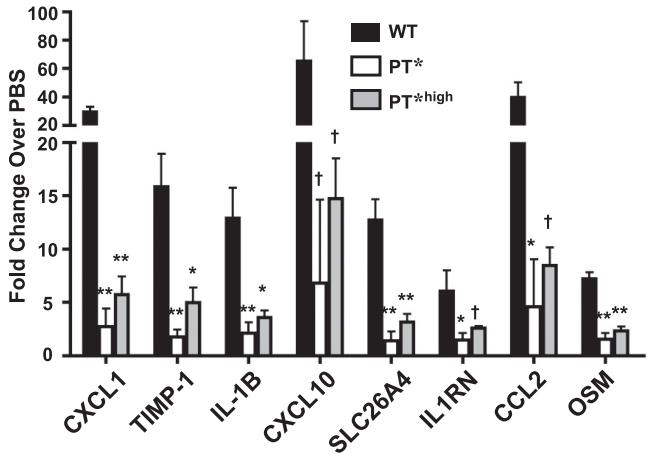

FIG 4 PT-associated upregulation of inflammatory genes requires ADP-ribosylation activity. BALB/c mice ($n = 3$ to 4 per group) were intranasally inoculated with PBS, WT *B. pertussis* (7.5×10^5 CFU), or a *B. pertussis* strain that produces enzymatically inactive PT (PT*) (7.5×10^5 CFU). Another group of mice was inoculated with a higher dose (1.5×10^7 CFU) of PT* (PT*^{high}). Transcript abundances in the lung at 4 dpi were assayed by using qPCR and normalized to levels in PBS-treated mice. Error bars indicate standard deviations. **, $P < 0.001$; *, $P < 0.01$; †, $P < 0.05$ (significantly different from WT values).

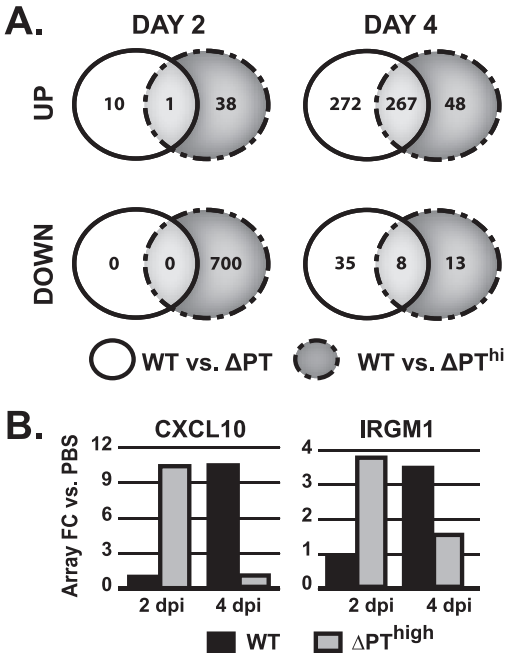

FIG 5 Time course of PT-associated gene regulation during *B. pertussis* infection. (A) Diagram showing genes differentially regulated in the mouse lung at 2 and 4 dpi. In a comparison of *X* versus *Y*, "UP" indicates genes expressed at higher levels in *X* than in *Y*, and "DOWN" refers to genes expressed at lower levels in *X* than in *Y*. Numbers indicate genes differentially expressed in the WT-versus-ΔPT comparison, the WT-versus-ΔPT^{high} comparison, or both comparisons (light gray), for probes with an FDR of <0.05 and a fold change of >1.5. (B) Examples of the reciprocal regulation patterns seen at 2 dpi in ΔPT^{high} infection versus PBS treatment and at 4 dpi in WT infection versus PBS treatment.

in WT- and ΔPT^{high}-infected mice between 1 and 4 dpi (Fig. 1B), a marked difference in the timing of transcriptional responses between these two infections was apparent (Table 1 and Fig. 5A). As mentioned above, robust changes in lung gene expression levels did not occur until 4 dpi in WT-infected mice. Indeed, a direct comparison of WT- and ΔPT-infected mice revealed only 11 differences at 2 dpi but 582 differences at 4 dpi (Table 1; see also Table S4 in the supplemental material). In contrast, ΔPT^{high}-infected mice showed an upregulation of a large number of genes at 2 dpi, many of which returned to near-background expression levels at 4 dpi. Three hundred twenty-seven of the genes with altered expression levels at 4 dpi in WT infection displayed near-equivalent regulation at 2 dpi in ΔPT^{high}-infected mice (in comparison to PBS-treated mice). These genes are listed in Table S7 in the supplemental material, and examples of the reciprocal regulation pattern are shown in Fig. 5B.

Two possibilities might explain these results. On the one hand, PT may have inhibited responses in WT infection that are elicited in the ΔPT^{high} infection at 2 dpi. Alternatively, responses in ΔPT^{high} infection at 2 dpi arose from higher bacterial loads (10^6 CFU) present from the outset in ΔPT^{high}-infected mice (Fig. 1B). Bacterial loads in WT-infected mice did not reach 10^6 CFU until 2 dpi, so if changes require a 2-day lag time, high-bacterial-load-induced gene regulation would not be detected until 4 dpi, as observed in our experiment. To distinguish between these possibilities, we compared lung transcriptional responses in mice inoculated with equally high doses of WT and PT-deficient strains (4×10^7 CFU for WT^{high} versus ΔPT^{high} infection). We reasoned that if high bacterial loads cause temporal differences in changes in gene expression levels, there should be no differences, or possibly greater responses in WT^{high}-infected mice, at 2 dpi. In contrast, if PT production inhibits responses at 2 dpi, WT^{high}-infected mice would display lower fold changes in gene expression levels than those observed for ΔPT^{high}-infected mice.

A comparison of gene expression changes at 2 dpi between WT^{high} and ΔPT^{high} infections revealed distinct patterns for different genes (Fig. 6A). Two out of nine genes (IL-6 and OSM) were expressed at higher levels in WT^{high}-infected mice, indicating that PT likely contributes to the increased expression levels of these genes, consistent with data from a previous report in the case of IL-6 (19). Six out of nine genes showed no significant difference in expression levels between WT^{high}- and ΔPT^{high}-infected mice, consistent with a correlation with early bacterial loads. The remaining gene (IFN-γ) was expressed at significantly lower levels in WT^{high}-infected mice, indicating that PT may inhibit its expres-

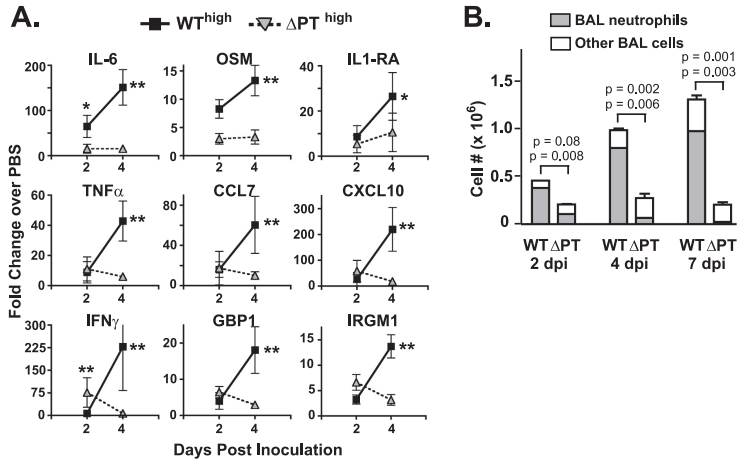

FIG 6 Comparison of responses in WT^{high} and ΔPT^{high} infections. Mice were inoculated with a high dose of either the WT or ΔPT *B. pertussis* strain ($n = 4$ per group). (A) Gene expression levels were measured in whole lung tissue at 2, 4, and 7 dpi. *, $P < 0.05$; **, $P < 0.001$. (B) Total cells and neutrophils from BAL fluid collected at 2, 4, and 7 dpi. Significant differences reflect total cell numbers (top) and neutrophil counts (bottom).

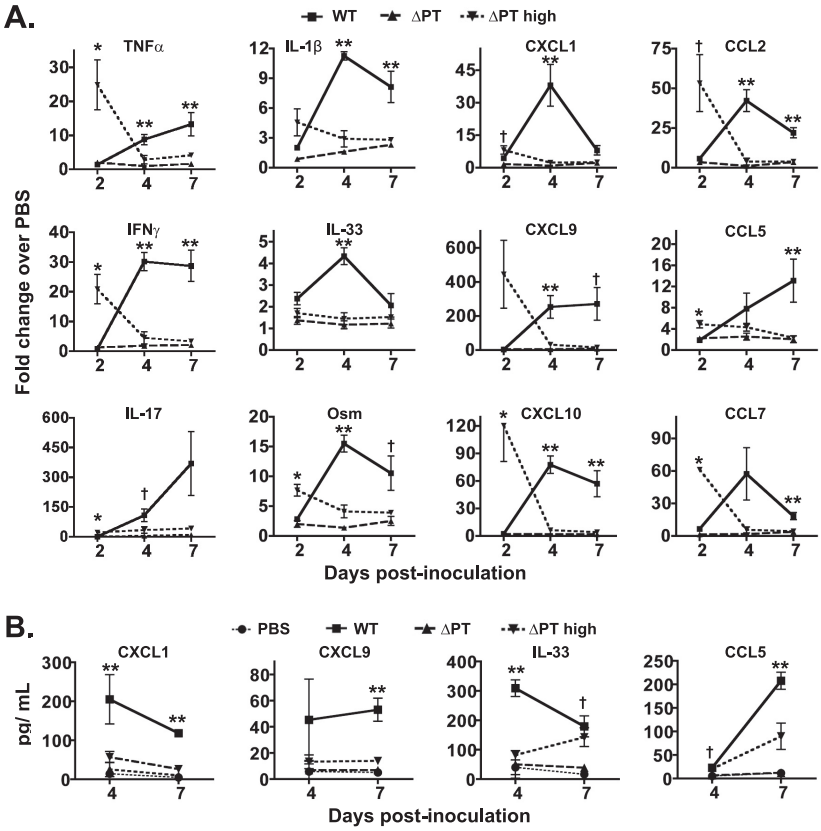

FIG 7 Increased and sustained cytokine and chemokine expression levels associated with PT in the lungs of *B. pertussis*-infected mice. (A) WT- or ΔPT-infected lungs were screened for cytokine and chemokine gene expression by qPCR at 2, 4, and 7 dpi (RNA samples from infection shown in Fig. 1). Changes in gene expression levels were normalized to values for PBS-treated mice. (B) In a separate experiment using a similar inoculation strategy as that described in the legend of Fig. 1, cytokine and chemokine levels were detected by ELISAs of mouse lung tissue harvested at 4 and 7 dpi. Significantly different ($P < 0.05$) values were detected for ΔPT^{high} versus WT and ΔPT infections (∗), WT versus ΔPT and ΔPT^{high} infections (∗∗), and either WT or ΔPT^{high} infection versus ΔPT infection (†).

sion at this early time point. By 4 dpi, all nine genes were expressed at significantly higher levels in WT^{high}-infected mice (Fig. 6A), consistent with either induction associated with PT activity or the higher bacterial loads in WT^{high}-infected mice at 2 dpi. Therefore, a combination of effects likely contributed to the difference in the timing of transcriptional responses between WT and ΔPT^{high} infections in the original experiment. The time course of bacterial loads likely influenced the timing of the changes in expression levels for most of the 327 genes, with inhibition by PT delaying the expression of a smaller subset until 4 dpi in WT infection. Such bacterial-load-driven patterns of increased gene expression levels in response to WT infection may be ascribed as indirectly associated with the presence of PT, in light of the function of PT to promote increased bacterial numbers during *B. pertussis* infection in this model (17).

Immune and inflammatory cells recruited to the lung during infection may contribute to the observed changes in gene expression levels and may explain some of the differences between WT- and ΔPT-infected mice. As such, we assessed total cell and neutrophil numbers in the airways (BAL fluid) of WT^{high}- and ΔPT^{high}-infected mice (Fig. 6B). At 2 dpi, WT^{high}-infected mice had ~2-fold more total cells and neutrophils than did ΔPT^{high}-infected mice. Thus, at this early time point, it is unlikely that such a modest difference in numbers of recruited cells contributed greatly to the overall differences in lung gene expression levels. At 4 and 7 dpi, more pronounced differences were observed. WT^{high} infection induced an influx of higher total cell numbers as well as >10-fold more neutrophils than did ΔPT^{high} infection. In this experiment, neutrophil numbers in ΔPT^{high}-infected mouse lungs at 2 dpi were 4- to 5-fold higher than the numbers that we previously reported for WT-infected mice at this time point but were not significantly different at 4 dpi. Our analysis of PT-associated genes (Table 1) did not identify an enrichment of neutrophil-specific genes, so neutrophil recruitment is unlikely to have been a major contributor to the PT-associated differential gene expression at 4 dpi.

Sustained expression of inflammatory genes in the presence of PT. Since we previously observed that certain cytokine gene expression levels peaked at 7 dpi in WT-infected mice (5), we hypothesized that the effects of PT on WT *B. pertussis* infection would sustain inflammatory gene expression beyond 4 dpi, versus the early and transient upregulation induced by ΔPT^{high} infection. Samples from WT-, ΔPT-, and ΔPT^{high}-infected mice at 2, 4, and 7 dpi were assayed by qPCR for the expression of several cytokines and chemokines to determine if the WT infection-induced gene upregulation observed at 4 dpi was maintained through 7 dpi. At 2 and 4 dpi, qPCR measurements confirmed the patterns of gene expression observed in the array data (Fig. 7A). In addition, the results showed that at 7 dpi in WT infection, transcripts for genes encoding TNF-α, IFN-γ, IL-1β, IL-17, CXCL9, CXCL10, CCL2,

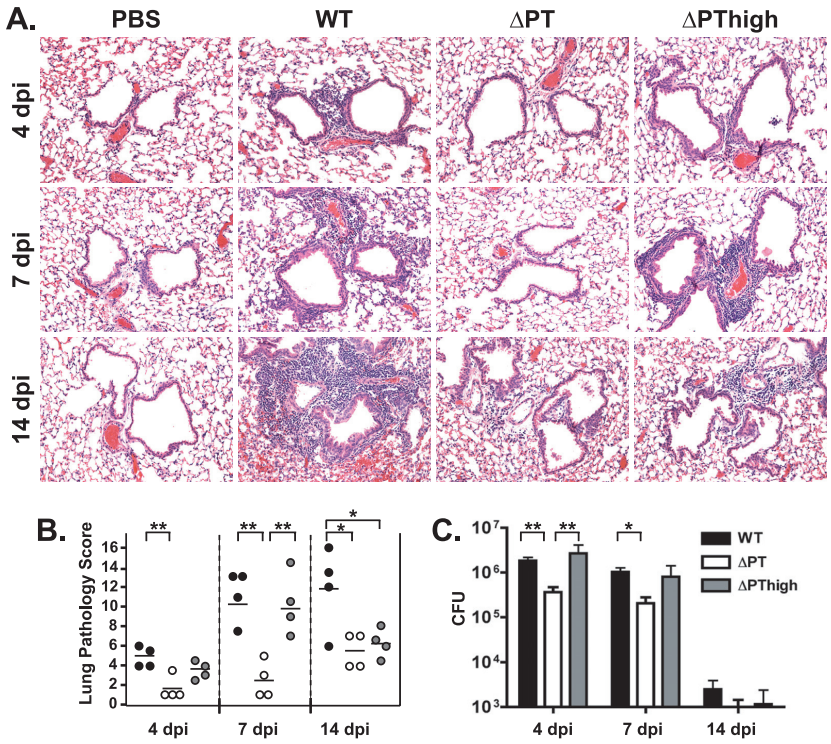

FIG 8 PT promotes sustained inflammation in the lungs of *B. pertussis*-infected mice. (A) Fixed lung tissue sections (5 μm) from mice inoculated with PBS or the WT, ΔPT, or ΔPT^{high} *B. pertussis* strain (4 mice per group) were stained with hematoxylin and eosin. Representative pictures from each strain at each time point are shown. Magnification, ×20. (B) Pathology scores of lung sections were assigned by a pathologist blinded to the experimental treatment. (C) Mean bacterial numbers recovered from lungs for each group. Legend colors apply to panels B and C. **, $P < 0.01$; *, $P < 0.05$.

CCL5, and CCL7 were maintained at levels significantly above the levels in ΔPT- and ΔPT^{high}-infected mice (Fig. 7A). In WT-infected mice, genes encoding TNF-α, IL-17, CXCL9, and CCL5 displayed higher expression levels at 7 dpi than at 4 dpi. Of note, several of these genes displayed the reciprocal regulation pattern discussed above (upregulation in ΔPT^{high}-infected mice at 2 dpi and upregulation to similar levels in WT-infected mice at 4 dpi). The observation that ΔPT^{high}-induced expression subsides by 4 dpi yet the WT-induced expression levels remain high at 7 dpi further supports the idea that, in WT infection, PT prolongs inflammatory responses elicited by sufficient bacterial loads in the airways.

To further validate some of these findings, we assayed lung homogenates from infected mice for levels of CXCL1, IL-33, CXCL9, and CCL5 by ELISAs (Fig. 7B). At 4 dpi, levels of CXCL1 and IL-33 were significantly higher in samples from WT *B. pertussis* infection than from the other infections. By 7 dpi, levels of CXCL1, CXCL9, and CCL5 were significantly higher in WT-infected mice, while IL-33 levels declined to those observed for samples from ΔPT^{high}-infected mice. Together, these results further validate the array data and demonstrate that PT plays a role in prolonged inflammatory gene expression in the airways of *B. pertussis*-infected mice.

Prolonged inflammatory pathology in the lungs of WT-infected mice. We next investigated whether the PT-associated expression of inflammatory genes at 4 and 7 dpi correlated with extended inflammatory pathology in the lungs of WT-infected mice. Lung tissue from mice infected with the WT, ΔPT, or ΔPT^{high} strain was isolated at 4, 7, and 14 dpi, and lung sections were evaluated for pathology. Representative views of lung sections from each infection are shown in Fig. 8A. Scores were assigned by a pathologist who was blinded to experimental treatment to measure changes in the following categories: bronchiolar inflammation, vessel inflammation, epithelial cell damage, hemorrhage, and numbers of eosinophils, neutrophils, macrophages, and leukocytes (Fig. 8B). At 4 dpi, lungs from all three infections showed only mild changes compared to lungs from mock-infected mice, including slight perivascular inflammation in WT and ΔPT^{high} infections, reflecting an influx of neutrophils and lymphocytes (Fig. 8A). By 7 dpi, moderate perivascular and mild peribronchiolar inflammation were apparent in both WT- and ΔPT^{high}-infected mice, with a slight indication of hemorrhage in all of the WT-infected mice and half of the latter. In addition, macrophage influx increased at this time point, possibly reflecting a recruitment of monocytes by the upregulated chemokines CCL2 and CCL7 (monocyte chemotactic proteins 1 and 3, respectively) (Fig. 7A). At 14 dpi, WT-infected lungs showed increased inflammation compared to that at 7 dpi (Fig. 8A and B), despite significant bacterial clearance from the lungs by this time point (Fig. 8C). Slight epithelial cell damage was noted, as were hemorrhage and an influx of neutrophils, lymphocytes, and macrophages. In contrast, the level of inflammation in ΔPT^{high}-infected mice declined by 14 dpi to levels observed for ΔPT-infected mice (Fig. 8A and B). These results show that an important effect of PT is to enhance and prolong airway inflammatory pathology during *B. pertussis* infection. Although an upregulation of inflammatory genes occurs by 4 dpi in WT infection, significant inflammatory

pathology in the lung becomes apparent only by 7 dpi and increases further at 14 dpi.

PT administration prolongs inflammatory pathology in ΔPT^{high}-infected mice. We reasoned that if PT enhances airway inflammation and pathology during *B. pertussis* infection, the airway administration of purified PT to ΔPT^{high}-infected mice should delay the resolution of inflammation and result in more intense, longer-lived inflammatory responses. Therefore, we inoculated mice with a high dose of the ΔPT strain, administered purified PT 24 h later (100 ng i.n.), and tested the effects of this treatment on subsequent airway inflammatory responses during infection. Control ΔPT^{high}-infected mice were treated with PBS at 24 h postinoculation, and other control mice were treated with PT without bacterial infection. PT administration at 24 h postinoculation did not significantly increase bacterial numbers in these mice (Fig. 9A), similarly to previously reported findings (17). Lung transcriptional responses were assayed at 3 and 7 dpi and showed that PT administration significantly increased the expression levels of TNF-α, CCL2, and CXCL10 in ΔPT^{high}-infected mice (Fig. 9B). In addition, histopathology analysis revealed exacerbated airway pathology at 7 and 14 dpi in ΔPT^{high}-infected mice treated with PT (Fig. 9C). PT treatment without bacterial infection did not significantly increase levels of inflammatory gene expression or pathology (data not shown). These data support the hypothesis that PT enhances and prolongs inflammatory gene expression and pathology during *B. pertussis* infection independently of bacterial loads. The data also demonstrate the long-lived effect of a single dose of PT in this model, as we observed previously (17, 18).

DISCUSSION

In this study, we used microarray technology to measure global lung gene expression changes associated with PT during *B. pertussis* infection in a mouse model, to assess the role of this toxin in modulating host airway responses, and to identify possible links between PT and *B. pertussis*-induced respiratory pathology. We compared infections by wild-type (PT-producing) and PT-deficient strains, and to control for the different bacterial loads achieved by these strains at the peak of infection, we also made comparisons to mice infected with a higher dose of the PT-deficient strain, which equalizes the bacterial loads (between the WT and ΔPT strains) at the peak of infection. By this approach, the differential expression of genes between WT infection and infection with either dose of the ΔPT strain identified potential PT-associated genes. By eliminating genes whose expression was apparently dependent on the timing of high bacterial loads rather than on PT, we identified a list of 91 genes whose altered expression levels can confidently be associated with PT production during *B. pertussis* infection. Data from this analysis and subsequent experiments demonstrated several important effects of PT during this bacterial infection: (i) PT plays an important role in altering airway gene expression in response to this infection, primarily through the upregulation of genes toward the peak of infection; (ii) immune and inflammatory responses dominated the most significant functional categories regulated by PT, with several cytokines and chemokines being among the most highly upregulated genes at the peak of *B. pertussis* infection; (iii) several other highly induced genes associated with PT are linked with pathology in the airways and other tissues; (iv) PT was associated with increased and sustained inflammatory gene expression levels and airway pathology through the peak of *B. pertussis* infection; and (v) PT administration heightened and prolonged inflammatory pathology associated with infection by a PT-deficient *B. pertussis* strain. Together, these data indicate that PT plays an important role in exacerbating pertussis airway disease pathology through the modulation of gene expression, in addition to other direct effects on host responses.

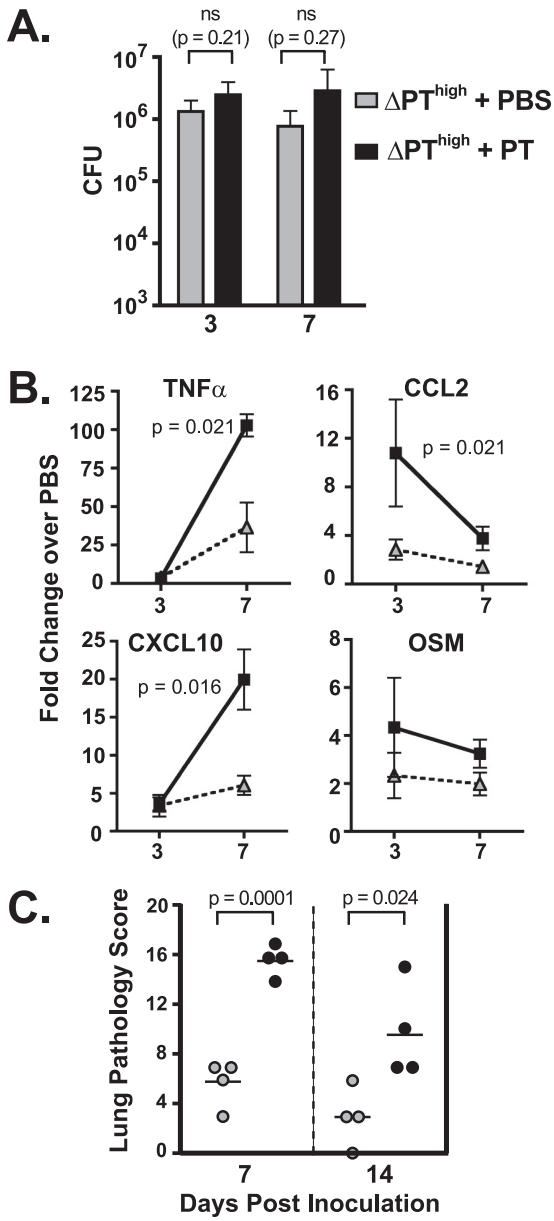

FIG 9 PT treatment exacerbates inflammation in ΔPT^{high}-infected mice. Mice were inoculated with a high dose of the ΔPT strain and treated with either PBS or 100 ng PT at 24 h postinoculation ($n = 4$ per group). PT treatment did not significantly increase lung bacterial loads (A) but was associated with elevated cytokine and chemokine transcript levels (B) and heightened lung pathology (C).

Our results comparing WT-infected to mock-infected mice are similar to those of a previously reported microarray analysis of wild-type *B. pertussis*-infected mouse lungs (using C3H mice and a higher dose of bacteria), in which a total of 1,841 genes (out of

22,000 tested) were differentially regulated (FDR < 0.05) at 1, 3, or 5 dpi (7). In that study, the response peaked at day 3 but was still high at day 5, and the majority of upregulated genes were involved in immune and inflammatory responses. In comparison, the total number of genes (out of ~24,000 tested) regulated in the WT infection in our study without regard to fold change equaled 3,737 (FDR ≤ 0.05). The higher number of regulated genes in our study may be related to the age or strain of mice or a greater sensitivity of our assay system.

Previously, we found that the expression of certain inflammatory cytokine and chemokine genes was upregulated in *B. pertussis* WT-infected mouse lungs at 4 dpi but not in ΔPT-infected mice (5), implicating PT in this response. The broadly important role of PT in upregulating multiple inflammatory responses to *B. pertussis* at the peak of infection was a major finding in the present study, in which a comparison of WT-infected to ΔPT- and ΔPT^{high}-infected mice identified immune and inflammatory responses as the most significantly upregulated functions. As well as previously identified upregulated cytokines and chemokines, such as KC (CXCL-1), IL-6, IFN-γ, and TNF-α, our study also revealed the PT-associated upregulation of cytokines such as IL-33 and oncostatin M, which were not previously reported in association with *B. pertussis* infection. These cytokines play roles in tissue damage and repair in the airways (50, 61) and may be involved in similar activities during *B. pertussis* infection.

The upregulation of cytokine and chemokine expression in the lungs raises the possibility that the presence of recruited immune and inflammatory cells contributes to the overall gene expression profile and differences between WT- and ΔPT-infected mice. Neutrophil numbers in the airways were not dramatically different between WT- and ΔPT^{high}-infected mice, and likewise, there was no enrichment of neutrophil-specific genes among the PT-associated genes. However, differences in other recruited cells may contribute to PT-associated gene expression. Future investigations could broadly address this question by assaying genome-wide expression profiles specifically in BAL fluid cell populations isolated from WT- or ΔPT-infected mice. It is likely that the majority of PT-associated responses occur in resident cells of the lung tissue exposed to the bacteria. The identification of which cells are responsible for specific gene expression differences would be a complex task, but we aim to investigate the specific cellular expression of at least a small number of genes that may contribute significantly to pertussis pathology.

For several cytokines and chemokines, we showed that the PT-associated upregulation of gene expression was sustained through 7 dpi and that differential gene expression correlated with protein production in lung tissue. These sustained effects of PT were reflected in the histopathology of infected lung tissue, with the highest levels being observed for WT-infected mice at 14 dpi. At 7 dpi, lung pathology was greater for WT-infected than for ΔPT-infected mice, consistent with data from a previous report (38), but ΔPT^{high}-infected mice had a level of pathology similar to that of WT-infected mice, presumably reflecting the earlier and more transient inflammatory responses observed for the ΔPT^{high} infection. The treatment of ΔPT^{high}-infected mice with purified PT increased inflammatory gene expression levels and prolonged airway pathology without significantly increasing bacterial loads. Since a similar treatment of uninfected mice with PT did not elicit inflammatory responses, this demonstrates that PT contributes significantly to the overall pathology in pertussis airway disease through an exacerbation of host responses to infection.

In addition to the multitude of upregulated inflammatory genes and pathways associated with PT contributing to airway pathology, other genes potentially associated with airway pathology were also highly upregulated by PT. One such gene encodes the membrane transporter SLC26A4 (pendrin), which participates in anion exchange at the apical surface of epithelial cells and negatively affects the volume of airway surface liquid (ASL) (58). ASL provides hydration around cilia, allowing proper ciliary beating, and thus plays an essential role in airway clearance. Pendrin overexpression increased inflammation and mucus production in asthma and chronic obstructive pulmonary disease (COPD) models (59) and potentiated allergen-induced airway hyperresponsiveness (AHR) in asthma (58), suggesting that it could play a role in AHR and cough in pertussis. In the kidney, pendrin can affect epithelial sodium channel (ENaC) activity and modulate the ENaC response to hormones that regulate blood pressure (83), and therefore, it is tempting to speculate that the altered pendrin regulation of ENaC in pertussis infection contributes to the pulmonary hypertension observed in lethal pertussis infections of infants (62). In addition, some serine proteases affect ENaC activation and ASL volume control, suggesting that specific serine protease inhibitors, including members of the SERPIN family, could participate in the regulation of ENaC activity (29). Two SERPIN protease inhibitors were among the other pathology-related genes identified as being PT upregulated in our study.

The inclusion of the ΔPT^{high} infection in this analysis revealed interesting differences from WT infection in the time course of responses despite equivalent bacterial loads at 2 and 4 dpi. At 2 dpi, responses peaked in the ΔPT^{high} infection, while responses to WT infection were still relatively modest. However, at 4 dpi, there was a broad response to WT infection, while most responses to ΔPT^{high} infection had returned to background levels. Numerous genes showed this reciprocal regulation pattern (see Table S7 in the supplemental material). To determine whether this was related to PT activity or to the higher dose and earlier bacterial loads of the ΔPT^{high} infection, we compared WT^{high} and ΔPT^{high} infections at these time points. The data indicated that the majority of the higher-level responses to ΔPT^{high} infection (than the responses to WT infection at the regular dose) were due to the earlier high bacterial loads achieved after the high initial dose. However, PT also appeared to inhibit the expression of a small number of genes at 2 dpi, and we cannot rule out the possibility that the PT inhibition of gene expression is more substantial at this time point. Although these data demonstrate that PT is not absolutely necessary for many of these responses, in a natural infection, the initial inoculum is likely to be relatively small and would require significant growth of the bacteria in the airways, which would require PT activity. In addition, the transient nature of the responses to ΔPT^{high} infection versus the greater and more prolonged responses to WT infection indicates that PT plays a role in sustaining many of the bacterial-load-induced responses. The mechanisms by which PT achieves these effects is not clear, but our data demonstrate that its ADP-ribosylation activity is required. One possibility is that PT activity inhibits host mechanisms to attenuate and resolve inflammation that occur after the initiation of infection. A candidate target for PT in this effect might be the sphingosine-1-phosphate (S1P) signaling pathway, since S1P receptors are PT-sensitive G-protein-coupled receptors

(GPCRs) (42). S1P signaling has been shown to attenuate acute lung injury induced by the intratracheal administration of LPS to mice (63) and can alleviate experimental allergic airway inflammation in mice (46). Recently, signaling specifically through S1P receptor 1 ($S1P_1$) was shown to suppress the pulmonary cytokine storm after influenza virus infection in mice, and endothelial cells were found to be the target of this activity (79). S1P signaling is known to enhance pulmonary endothelial barrier function (24). Therefore, the PT inhibition of $S1P_1$ signaling on the pulmonary endothelium may cause vascular leakage into the airways and promote increased levels of cytokine and chemokine production, characteristics of peak pertussis infection in the mouse model. In addition, several endogenous lipid mediators of the resolution of inflammation (resolvins and lipoxins) act through PT-sensitive GPCRs (43, 80), and therefore, PT may mediate sustained inflammatory responses by the inhibition of these mechanisms as well.

It is likely that not all of the effects of PT on host responses and pathology would be identified by changes in gene expression, since PT may act more directly on GPCR signaling pathways to induce pathology. Several PT-sensitive GPCRs are involved in inflammatory processes, such as chemokine, leukotriene, and prostaglandin receptors. In addition, a recent report outlined one possible mechanism by which PT might exacerbate cough responses, by inhibiting the desensitization of bradykinin receptors (34). Bradykinin, a peptide implicated in airway inflammatory diseases (1), signals through the activation of bradykinin B2 receptors, GPCRs that couple with both G_q and G_i (44). Preliminary data indicate that PT (but not PT*) inhibits B2 receptor desensitization in guinea pig vagal sensory neurons regulating bradykinin-evoked cough (34), which may correlate with the paroxysmal nature (inability to stop coughing) of pertussis cough episodes.

Currently, no effective treatment for pertussis exists. With an increasing rate of pertussis infection despite widespread vaccination, there is clearly a need for a further understanding of the molecular mechanisms of pertussis pathogenesis. By demonstrating the robust, PT-associated exacerbation of airway inflammation and pathology, this study emphasizes the importance of PT as a critical virulence factor of *B. pertussis*. Further work in this direction may reveal novel targets for therapeutic intervention in pertussis patients, which may alleviate the severe and prolonged cough and reduce the rate of transmission of this disease.

ACKNOWLEDGMENTS

We extend thanks to the following individuals: Jing Yin and Li Tang (UMB Biopolymer Core Facility) for the preparation of cRNA and array hybridizations; Susan Dorsey for assistance with array data management; Michael Lipsky for pathology scores; Matthew Frieman for critical reading of the manuscript prior to submission; and Carbonetti laboratory members, Carlo Colantuoni, and Stefanie Vogel for helpful discussions.

This work was supported by NIH grant AI063080 to N.H.C.

C.E.C. and N.H.C. conceived of and designed the experiments. Y.S. normalized and carried out statistical analysis of microarray data. C.E.C. performed the experiments. C.E.C. and N.H.C. analyzed the data. C.E.C. and N.H.C. wrote the paper.

REFERENCES

1. **Abraham WM, Scuri M, Farmer SG.** 2006. Peptide and non-peptide bradykinin receptor antagonists: role in allergic airway disease. Eur. J. Pharmacol. **533**:215–221.
2. **Agarwal RK, Sun SH, Su SB, Chan CC, Caspi RR.** 2002. Pertussis toxin alters the innate and the adaptive immune responses in a pertussis-dependent model of autoimmunity. J. Neuroimmunol. **129**:133–140.
3. **Alfano M, Schmidtmayerova H, Amella CA, Pushkarsky T, Bukrinsky M.** 1999. The B-oligomer of pertussis toxin deactivates CC chemokine receptor 5 and blocks entry of M-tropic HIV-1 strains. J. Exp. Med. **190**: 597–605.
4. **Andreasen C, Carbonetti NH.** 2008. Pertussis toxin inhibits early chemokine production to delay neutrophil recruitment in response to Bordetella pertussis respiratory tract infection in mice. Infect. Immun. **76**:5139–5148.
5. **Andreasen C, Powell DA, Carbonetti NH.** 2009. Pertussis toxin stimulates IL-17 production in response to Bordetella pertussis infection in mice. PLoS One **4**:e7079. doi:10.1371/journal.pone.0007079.
6. **Angelini DJ, et al.** 2009. Resistin-like molecule-beta in scleroderma-associated pulmonary hypertension. Am. J. Respir. Cell Mol. Biol. **41**:553–561.
7. **Banus S, et al.** 2007. Lung response to Bordetella pertussis infection in mice identified by gene-expression profiling. Immunogenetics **59**:555–564.
8. **Barksby HE, Lea SR, Preshaw PM, Taylor JJ.** 2007. The expanding family of interleukin-1 cytokines and their role in destructive inflammatory disorders. Clin. Exp. Immunol. **149**:217–225.
9. **Benjamini Y, Drai D, Elmer G, Kafkafi N, Golani I.** 2001. Controlling the false discovery rate in behavior genetics research. Behav. Brain Res. **125**:279–284.
10. **Bouchez V, et al.** 2009. First report and detailed characterization of B. pertussis isolates not expressing pertussis toxin or pertactin. Vaccine **27**: 6034–6041.
11. **Brabb T, et al.** 1997. Triggers of autoimmune disease in a murine TCR-transgenic model for multiple sclerosis. J. Immunol. **159**:497–507.
12. **Buc M, Dzurilla M, Vrlik M, Bucova M.** 2009. Immunopathogenesis of bronchial asthma. Arch. Immunol. Ther. Exp. (Warsz.) **57**:331–344.
13. **Carballo E, Lai WS, Blackshear PJ.** 1998. Feedback inhibition of macrophage tumor necrosis factor-alpha production by tristetraprolin. Science **281**:1001–1005.
14. **Carbonetti NH.** 2010. Pertussis toxin and adenylate cyclase toxin: key virulence factors of Bordetella pertussis and cell biology tools. Future Microbiol. **5**:455–469.
15. **Carbonetti NH, Artamonova GV, Andreasen C, Bushar N.** 2005. Pertussis toxin and adenylate cyclase toxin provide a one-two punch for establishment of Bordetella pertussis infection of the respiratory tract. Infect. Immun. **73**:2698–2703.
16. **Carbonetti NH, et al.** 2004. Suppression of serum antibody responses by pertussis toxin after respiratory tract colonization by Bordetella pertussis and identification of an immunodominant lipoprotein. Infect. Immun. **72**:3350–3358.
17. **Carbonetti NH, Artamonova GV, Mays RM, Worthington ZE.** 2003. Pertussis toxin plays an early role in respiratory tract colonization by Bordetella pertussis. Infect. Immun. **71**:6358–6366.
18. **Carbonetti NH, Artamonova GV, Van Rooijen N, Ayala VI.** 2007. Pertussis toxin targets airway macrophages to promote Bordetella pertussis infection of the respiratory tract. Infect. Immun. **75**:1713–1720.
19. **Chen X, Howard OM, Oppenheim JJ.** 2007. Pertussis toxin by inducing IL-6 promotes the generation of IL-17-producing CD4 cells. J. Immunol. **178**:6123–6129.
20. **Chen X, et al.** 2006. Pertussis toxin as an adjuvant suppresses the number and function of CD4+CD25+ T regulatory cells. Eur. J. Immunol. **36**: 671–680.
21. **Choi KH, et al.** 2002. The role of matrix metalloproteinase-9 and tissue inhibitor of metalloproteinase-1 in cryptogenic organizing pneumonia. Chest **121**:1478–1485.
22. **Cyster JG, Goodnow CC.** 1995. Pertussis toxin inhibits migration of B and T lymphocytes into splenic white pulp cords. J. Exp. Med. **182**:581–586.
23. **Dittrich AM, et al.** 2010. Lipocalin2 protects against airway inflammation and hyperresponsiveness in a murine model of allergic airway disease. Clin. Exp. Allergy **40**:1689–1700.
24. **Dudek SM, et al.** 2004. Pulmonary endothelial cell barrier enhancement by sphingosine 1-phosphate: roles for cortactin and myosin light chain kinase. J. Biol. Chem. **279**:24692–24700.
25. **Dunning MJ, Smith ML, Ritchie ME, Tavare S.** 2007. beadarray: R classes and methods for Illumina bead-based data. Bioinformatics **23**: 2183–2184.
26. **Eyles JL, Roberts AW, Metcalf D, Wicks IP.** 2006. Granulocyte colony-

stimulating factor and neutrophils—forgotten mediators of inflammatory disease. Nat. Clin. Pract. Rheumatol. **2**:500–510.
27. **Fang C, et al.** 2012. Resistin-like molecule-beta is a human airway remodelling mediator. Eur. Respir. J. **39**:458–466.
28. **Flo TH, et al.** 2004. Lipocalin 2 mediates an innate immune response to bacterial infection by sequestrating iron. Nature **432**:917–921.
29. **Gaillard EA, et al.** 2010. Regulation of the epithelial Na+ channel and airway surface liquid volume by serine proteases. Pflugers Arch. **460**:1–17.
30. **Garantziotis S, et al.** 2007. Inter-alpha-trypsin inhibitor attenuates complement activation and complement-induced lung injury. J. Immunol. **179**:4187–4192.
31. **Goodwin MS, Weiss AA.** 1990. Adenylate cyclase toxin is critical for colonization and pertussis toxin is critical for lethal infection by Bordetella pertussis in infant mice. Infect. Immun. **58**:3445–3447.
32. **Hassoun PM.** 2009. Pulmonary arterial hypertension complicating connective tissue diseases. Semin. Respir. Crit. Care Med. **30**:429–439.
33. **He Q, Mertsola J.** 2008. Factors contributing to pertussis resurgence. Future Microbiol. **3**:329–339.
34. **Hewitt M, Canning BJ.** 2010. Coughing precipitated by Bordetella pertussis infection. Lung **188**(Suppl 1):S73–S79.
35. **Hofstetter HH, Luhder F, Toyka KV, Gold R.** 2006. IL-17 production by thymocytes upon CD3 stimulation and costimulation with microbial factors. Cytokine **34**:184–197.
36. **Jajoo S, Mukherjea D, Pingle S, Sekino Y, Ramkumar V.** 2006. Induction of adenosine A1 receptor expression by pertussis toxin via an adenosine 5′-diphosphate ribosylation-independent pathway. J. Pharmacol. Exp. Ther. **317**:1–10.
37. **Katada T, Tamura M, Ui M.** 1983. The A protomer of islet-activating protein, pertussis toxin, as an active peptide catalyzing ADP-ribosylation of a membrane protein. Arch. Biochem. Biophys. **224**:290–298.
38. **Khelef N, Bachelet CM, Vargaftig BB, Guiso N.** 1994. Characterization of murine lung inflammation after infection with parental Bordetella pertussis and mutants deficient in adhesins or toxins. Infect. Immun. **62**: 2893–2900.
39. **Kim BH, et al.** 2011. A family of IFN-gamma-inducible 65-kD GTPases protects against bacterial infection. Science **332**:717–721.
40. **Kim YH, et al.** 2011. 4-1BB triggering ameliorates experimental autoimmune encephalomyelitis by modulating the balance between Th17 and regulatory T cells. J. Immunol. **187**:1120–1128.
41. **Kirimanjeswara GS, Agosto LM, Kennett MJ, Bjornstad ON, Harvill ET.** 2005. Pertussis toxin inhibits neutrophil recruitment to delay antibody-mediated clearance of Bordetella pertussis. J. Clin. Invest. **115**: 3594–3601.
42. **Lee MJ, et al.** 1998. Sphingosine-1-phosphate as a ligand for the G protein-coupled receptor EDG-1. Science **279**:1552–1555.
43. **Maderna P, Godson C.** 2009. Lipoxins: resolutionary road. Br. J. Pharmacol. **158**:947–959.
44. **Maher SA, Dubuis ED, Belvisi MG.** 2011. G-protein coupled receptors regulating cough. Curr. Opin. Pharmacol. **11**:248–253.
45. **Maki JM, et al.** 2005. Lysyl oxidase is essential for normal development and function of the respiratory system and for the integrity of elastic and collagen fibers in various tissues. Am. J. Pathol. **167**:927–936.
46. **Marsolais D, Yagi S, Kago T, Leaf N, Rosen H.** 2011. Modulation of chemokines and allergic airway inflammation by selective local sphingosine-1-phosphate receptor 1 agonism in lungs. Mol. Pharmacol. **79**: 61–68.
47. **Martino A, Volpe E, Auricchio G, Colizzi V, Baldini PM.** 2006. Influence of pertussis toxin on CD1a isoform expression in human dendritic cells. J. Clin. Immunol. **26**:153–159.
48. **Mattoo S, Cherry JD.** 2005. Molecular pathogenesis, epidemiology, and clinical manifestations of respiratory infections due to Bordetella pertussis and other Bordetella subspecies. Clin. Microbiol. Rev. **18**:326–382.
49. **Millen SH, Lewallen DM, Herr AB, Iyer SS, Weiss AA.** 2010. Identification and characterization of the carbohydrate ligands recognized by pertussis toxin via a glycan microarray and surface plasmon resonance. Biochemistry **49**:5954–5967.
50. **Miller AM.** 2011. Role of IL-33 in inflammation and disease. J. Inflamm. (Lond.) **8**:22. doi:10.1186/1476-9255-8-22.
51. **Monticelli LA, et al.** 2011. Innate lymphoid cells promote lung-tissue homeostasis after infection with influenza virus. Nat. Immunol. **12**:1045–1054.
52. **Mooi FR, et al.** 2009. Bordetella pertussis strains with increased toxin production associated with pertussis resurgence. Emerg. Infect. Dis. **15**: 1206–1213.
53. **Morse SI, Morse JH.** 1976. Isolation and properties of the leukocytosis- and lymphocytosis-promoting factor of Bordetella pertussis. J. Exp. Med. **143**:1483–1502.
54. **Moss J, et al.** 1983. Activation by thiol of the latent NAD glycohydrolase and ADP-ribosyltransferase activities of Bordetella pertussis toxin (islet-activating protein). J. Biol. Chem. **258**:11879–11882.
55. **Mozaffarian A, et al.** 2008. Mechanisms of oncostatin M-induced pulmonary inflammation and fibrosis. J. Immunol. **181**:7243–7253.
56. **Munoz JJ, Arai H, Bergman RK, Sadowski PL.** 1981. Biological activities of crystalline pertussigen from Bordetella pertussis. Infect. Immun. **33**: 820–826.
57. **Munoz JJ, Bernard CC, Mackay IR.** 1984. Elicitation of experimental allergic encephalomyelitis (EAE) in mice with the aid of pertussigen. Cell. Immunol. **83**:92–100.
58. **Nakagami Y, et al.** 2008. The epithelial anion transporter pendrin is induced by allergy and rhinovirus infection, regulates airway surface liquid, and increases airway reactivity and inflammation in an asthma model. J. Immunol. **181**:2203–2210.
59. **Nakao I, et al.** 2008. Identification of pendrin as a common mediator for mucus production in bronchial asthma and chronic obstructive pulmonary disease. J. Immunol. **180**:6262–6269.
60. **Nasso M, et al.** 2009. Genetically detoxified pertussis toxin induces Th1/Th17 immune response through MAPKs and IL-10-dependent mechanisms. J. Immunol. **183**:1892–1899.
61. **O'Hara KA, Kedda MA, Thompson PJ, Knight DA.** 2003. Oncostatin M: an interleukin-6-like cytokine relevant to airway remodelling and the pathogenesis of asthma. Clin. Exp. Allergy **33**:1026–1032.
62. **Paddock CD, et al.** 2008. Pathology and pathogenesis of fatal Bordetella pertussis infection in infants. Clin. Infect. Dis. **47**:328–338.
63. **Peng X, et al.** 2004. Protective effects of sphingosine 1-phosphate in murine endotoxin-induced inflammatory lung injury. Am. J. Respir. Crit. Care Med. **169**:1245–1251.
64. **Petersen JW, Ibsen PH, Haslov K, Heron I.** 1992. Proliferative responses and gamma interferon and tumor necrosis factor production by lymphocytes isolated from tracheobroncheal lymph nodes and spleen of mice aerosol infected with Bordetella pertussis. Infect. Immun. **60**:4563–4570.
65. **Pizza M, et al.** 1989. Mutants of pertussis toxin suitable for vaccine development. Science **246**:497–500.
66. **Plaut RD, Carbonetti NH.** 2008. Retrograde transport of pertussis toxin in the mammalian cell. Cell. Microbiol. **10**:1130–1139.
67. **Ren Z, et al.** 2011. IRF-1 signaling in central nervous system glial cells regulates inflammatory demyelination. J. Neuroimmunol. **233**:147–159.
68. **Rowan AD, Hui W, Cawston TE, Richards CD.** 2003. Adenoviral gene transfer of interleukin-1 in combination with oncostatin M induces significant joint damage in a murine model. Am. J. Pathol. **162**:1975–1984.
69. **Sands MF, et al.** 2009. Tissue inhibitor of metalloproteinase-1 modulates allergic lung inflammation in murine asthma. Clin. Immunol. **130**:186–198.
70. **Scaffidi AK, et al.** 2002. Oncostatin M stimulates proliferation, induces collagen production and inhibits apoptosis of human lung fibroblasts. Br. J. Pharmacol. **136**:793–801.
71. **Schumacher C, Clark-Lewis I, Baggiolini M, Moser B.** 1992. High- and low-affinity binding of GRO alpha and neutrophil-activating peptide 2 to interleukin 8 receptors on human neutrophils. Proc. Natl. Acad. Sci. U. S. A. **89**:10542–10546.
72. **Shimada A, et al.** 2008. Reduced pulmonary function is associated with enhanced inflammation and tissue inhibitor of metalloproteinase 1 concentration in the bronchoalveolar lavage fluid of patients with lung parenchymal sarcoidosis. Kurume Med. J. **55**:13–17.
73. **Shumilla JA, et al.** 2004. Bordetella pertussis infection of primary human monocytes alters HLA-DR expression. Infect. Immun. **72**:1450–1462.
74. **Sipione S, et al.** 2006. Identification of a novel human granzyme B inhibitor secreted by cultured sertoli cells. J. Immunol. **177**:5051–5058.
75. **Smyth GK.** 2005. Limma: linear models for microarray data, p 397–420. *In* Gentleman VCR, Dudoit S, Irizarry R, Huber W (ed), Bioinformatics and computational biology solutions using R and Bioconductor. Springer, New York, NY.
76. **Spangrude GJ, Sacchi F, Hill HR, Van Epps DE, Daynes RA.** 1985. Inhibition of lymphocyte and neutrophil chemotaxis by pertussis toxin. J. Immunol. **135**:4135–4143.
77. **Tamura M, et al.** 1982. Subunit structure of islet-activating protein,

pertussis toxin, in conformity with the A-B model. Biochemistry **21**:5516–5522.
78. **Tamura M, Nogimori K, Yajima M, Ase K, Ui M.** 1983. A role of the B-oligomer moiety of islet-activating protein, pertussis toxin, in development of the biological effects on intact cells. J. Biol. Chem. **258**:6756–6761.
79. **Teijaro JR, et al.** 2011. Endothelial cells are central orchestrators of cytokine amplification during influenza virus infection. Cell **146**:980–991.
80. **Uddin M, Levy BD.** 2011. Resolvins: natural agonists for resolution of pulmonary inflammation. Prog. Lipid Res. **50**:75–88.
81. **Ui M, et al.** 1984. Islet-activating protein, pertussis toxin: a specific uncoupler of receptor-mediated inhibition of adenylate cyclase. Adv. Cyclic Nucleotide Protein Phosphorylation Res. **17**:145–151.
82. **Vogel FR, Klein TW, Stewart WE II, Igarashi T, Friedman H.** 1985. Immune suppression and induction of gamma interferon by pertussis toxin. Infect. Immun. **49**:90–97.
83. **Wall SM, Pech V.** 2008. The interaction of pendrin and the epithelial sodium channel in blood pressure regulation. Curr. Opin. Nephrol. Hypertens. **17**:18–24.
84. **Weaver CT, Harrington LE, Mangan PR, Gavrieli M, Murphy KM.** 2006. Th17: an effector CD4 T cell lineage with regulatory T cell ties. Immunity **24**:677–688.
85. **Weiss AA, Hewlett EL, Myers GA, Falkow S.** 1984. Pertussis toxin and extracytoplasmic adenylate cyclase as virulence factors of Bordetella pertussis. J. Infect. Dis. **150**:219–222.
86. **Witvliet MH, Burns DL, Brennan MJ, Poolman JT, Manclark CR.** 1989. Binding of pertussis toxin to eucaryotic cells and glycoproteins. Infect. Immun. **57**:3324–3330.
87. **World Health Organization.** 2011. Immunization, vaccines, and biologicals: pertussis. World Health Organization, Geneva, Switzerland. http://www.who.int/immunization/topics/pertussis/en/index.html.
88. **Yamagata T, Ichinose M.** 2006. Agents against cytokine synthesis or receptors. Eur. J. Pharmacol. **533**:289–301.
89. **Yamasaki S, et al.** 2008. Mincle is an ITAM-coupled activating receptor that senses damaged cells. Nat. Immunol. **9**:1179–1188.
90. **Zhang X, et al.** 2011. Interleukin-1 receptor signaling is required to overcome the effects of pertussis toxin and for efficient infection- or vaccination-induced immunity against Bordetella pertussis. Infect. Immun. **79**:527–541.
91. **Zhang X, Morrison DC.** 1993. Pertussis toxin-sensitive factor differentially regulates lipopolysaccharide-induced tumor necrosis factor-alpha and nitric oxide production in mouse peritoneal macrophages. J. Immunol. **150**:1011–1018.
92. **Zhao CB, et al.** 2008. A new EAE model of brain demyelination induced by intracerebroventricular pertussis toxin. Biochem. Biophys. Res. Commun. **370**:16–21.
93. **Zhao J, et al.** 2011. Lysophosphatidic acid receptor 1 modulates lipopolysaccharide-induced inflammation in alveolar epithelial cells and murine lungs. Am. J. Physiol. Lung Cell. Mol. Physiol. **301**:L547–L556. doi:10.1152/ajplung.0058.2011.